National Defence
Défense nationale

DESCRIPTION OF THE OHGR DATABASE

by

Anastasios Drosopoulos

DEFENCE RESEARCH ESTABLISHMENT OTTAWA
TECHNICAL NOTE 94-14

Canada

19950125 074

December 1994
Ottawa

National Défense
Defence nationale

DESCRIPTION OF THE OHGR DATABASE

by

Anastasios Drosopoulos
Airborne Radar and Navigation Section
Radar and Space Division

DTIC QUALITY INSPECTED 3

DEFENCE RESEARCH ESTABLISHMENT OTTAWA
TECHNICAL NOTE 94-14

PCN
021LA

December 1994
Ottawa

Abstract

This Technical Note describes the Osborne Head database, collected at Osborne Head Gunnery Range, OHGR, in November 1993, with the McMaster University IPIX radar, under contract to DSS. Representative examples are worked out for the different operational modes of the radar (staring, scanning, alternate/single polarization, single/multi frequency). Strengths and weaknesses of the database are pointed out as well. The purpose of this Technical Note is to serve as a guide to the database, presenting enough information to allow the extraction of individual datasets from the raw data. These can subsequently be used for sea clutter, target model validation and/or testing of signal processing techniques, leading to enhanced target detection in sea clutter.

Résumé

Cette Note Technique décrit la banque de données Osborne Head, recueillie au site expérimental Osborne Head Gunnery Range (OHGR) en novembre 1993, à l'aide du radar IPIX de l'université McMaster. Le travail fut réalisé sous contrat pour Approvisionnement et Services Canada. Des exemples représentatifs sont étudiés pour les différents modes d'opération du radar (fixe, balayage, polarisation unique/alternée, fréquence unique/multiple). La qualité de la banque de données est évaluée aussi. Cette Note Technique sert de guide d'utilisation de la banque de données. Elle présente suffisamment d'information pour permettre l'extraction de jeux de données individuels. Ces jeux peuvent ensuite être utilisés pour l'étude du fouillis de la mer, pour la validation de modèles de cible et pour l'évaluation de diverses techniques d'analyse de signaux, dans le but d'améliorer les capacités de détection de cibles dans le fouillis de la mer.

Executive Summary

This Technical Note describes the Osborne Head database, collected at Osborne Head Gunnery Range, OHGR, in November 1993, with the McMaster University IPIX radar, under contract to DSS. Representative examples are worked out for the different operational modes of the radar (staring, scanning, alternate/single polarization, single/multi frequency).

The strengths of the database include the dual polarized and frequency agile nature of the radar signals involved. The differences between the two polarizations can be seen in the data and the full polarization matrix can be constructed. With frequency agility the potential exists to synthesize a high resolution range profile thus improving the radar range resolution. The preliminary processing carried out in this report has also brought out a "weakness" of the database. Data clipping is observed in several datasets, due to the fact that the gain control at the receiver is not properly set during data collection. Although this could make such datasets useless for some applications, they offer an opportunity to investigate the deterioration commonly observed in operational radars due exactly to this effect. A future report, in preparation, is examining the points mentioned above, together with a careful examination of the sea clutter statistics.

The database, including all operational and ground-truthing data, can be made available to interested organizations in the form of 8mm Unix tar archived and compressed tapes. The purpose of this Tecnical Note is to serve as a guide to the database, presenting enough information to allow the extraction of individual datasets from the raw data. These can subsequently be used for sea clutter, target model validation and/or testing of signal processing techniques, leading to enhanced target detection in sea clutter.

Contents

List of Tables

List of Figures

1

Introduction

New problems have appeared in the area of target detection in sea clutter, with the introduction of high-resolution radars, made possible with today's technology. The expectation was that with the smaller sea surface area intercepted by the narrower radar pulse, the sea clutter would be less, leading to a significant detection improvement. It turned out that this improvement is not as great as expected since the sea clutter statistics are no longer Gaussian, the assumption that most radar signal processing hardware is based on.

There are basically two possible ways of characterizing sea clutter and finding out the actual sea clutter statistics. Radar engineers normally take the phenomenological approach, where empirical distributions of sea clutter are estimated, under typical radar operating conditions, with a certain category of radars. These distributions are then used to estimate radar detection performance.

The more straightforward approach is to look into the actual electromagnetic scattering mechanism from the sea surface in the microwave frequency regime. This is a much more complicated problem as the number of factors that affect the return signal can be prohibitively large and difficult to adequately model. The common route is to make simplifying approximations, e.g. tangent-plane, small-perturbation, two-scale composite model etc. The problem is that these approximations often do not adequately describe experimental observations in the regimes of interest for target detection in sea clutter. Interestingly enough, an old reference by Hasselmann [2] on the Bispectra of Ocean Waves, indicates the need to use at least 4th order statistics to model sea spikes, the prevalent problem in high resolution detection.

In order to confidently establish regions of validity for the various models employed, empirical or theoretical, a significant amount of model validation must be done with as large a variety

Table 1.1: IPIX radar parameters for OHGR trials

Transmitter
- 8 kW peak power TWT
- dual frequency simultaneous transmission, 8.9–9.4 GHz; fixed & agile
- H or V polarization; switchable pulse-to-pulse; 4 kHz max rate
- pulsewidth 20–5000 *ns*; normally used 200 *ns*
- PRF arbitrary; 100 *µs* minimum

Receivers
- coherent reception
- 2 linear receivers; H or V on each receiver
- tuned to fixed or agile frequency
- instantaneous dynamic range > 50 dB

Parabolic dish Antenna
- 2.4 m diameter
- pencil beam beamwidth 0.9°
- 44 dB antenna gain
- sidelobes < −30 dB
- cross-polarization isolation > 33 dB
- rotation rate 0–30 rpm

Table 1.2: The targets deployed for the OHGR trials

target name	date deployed	nominal azimuth (°)	nominal range (m)
targA	Nov 5	128°	2660
targB	Nov 5	130°	5525
dihed	Nov 5	223.7°	2438
trihed	Nov 5	223.3°	2355
targC	Nov 17	170°	2655

of different databases as possible. DREO is currently building up the technical and information background structure, that will lead to a better understanding of sea clutter and detection of targets in sea clutter in general. This understanding will eventually lead to the devising of signal processing techniques that improve the detection capabilities of CF radars.

A similar objective is held by the TTCP countries. The Radar Signal Processing Panel, KTP3 has approved the tasking of a study that will lead to the development of a sea clutter model that achieves it. In this collaboration, data and model information is to be exchanged and the database described in this report is available for this purpose. The present report is to be used as a guide in properly reading and calibrating the raw data.

This database is one more source in the library of databases to be investigated. It is collected with the McMaster University IPIX radar under contract to DSS (DSS contract W7714-3-9722/01-SV). This is an experimental, instrumentation class radar, capable of dual polarized and frequency agile operation (Table 1.1).

The radar site was located at 44°36.72′ N, 63°25.41′ W, on a cliff facing the Atlantic Ocean, at a height of 100 feet above mean sea level and an open ocean view of about 130° (Fig. 1.1).

A total of three small floating targets (beachballs containing a standard marine radar enhancer and covered with reflecting aluminum foil) and two reflectors (dihedral and trihedral) were deployed (Table 1.2).

The data of the OHGR datasets are stored as 1 byte integers from 0 to 255. There is a 1200 byte header and a 16 byte trailer in each dataset. The actual data order is shown in Fig. 1.2 for the most general case. There is always like polarization (Lpol) and cross polarization (Xpol) reception, leading to a quadruplet of I and Q values for Lpol and Xpol. A sequence of such quadruplets fills out the first loop for all the range bins available. At the end of this range bin sequence there is always an extra quadruplet of 255's indicating the sequence end. This must be removed when using the data.

When reading the raw data, if FORTRAN is employed, the open file and read statements should be similar to:

```
open(1,file="data_filename",status="old",access="direct",
&    form="unformatted", recl=1)

read(1,rec=irec) ibyte
```

where **ibyte** is a **byte** type variable. In C/C++, an **unsigned char** is used (one byte long) for reading, subsequently assigned to an **unsigned int**.
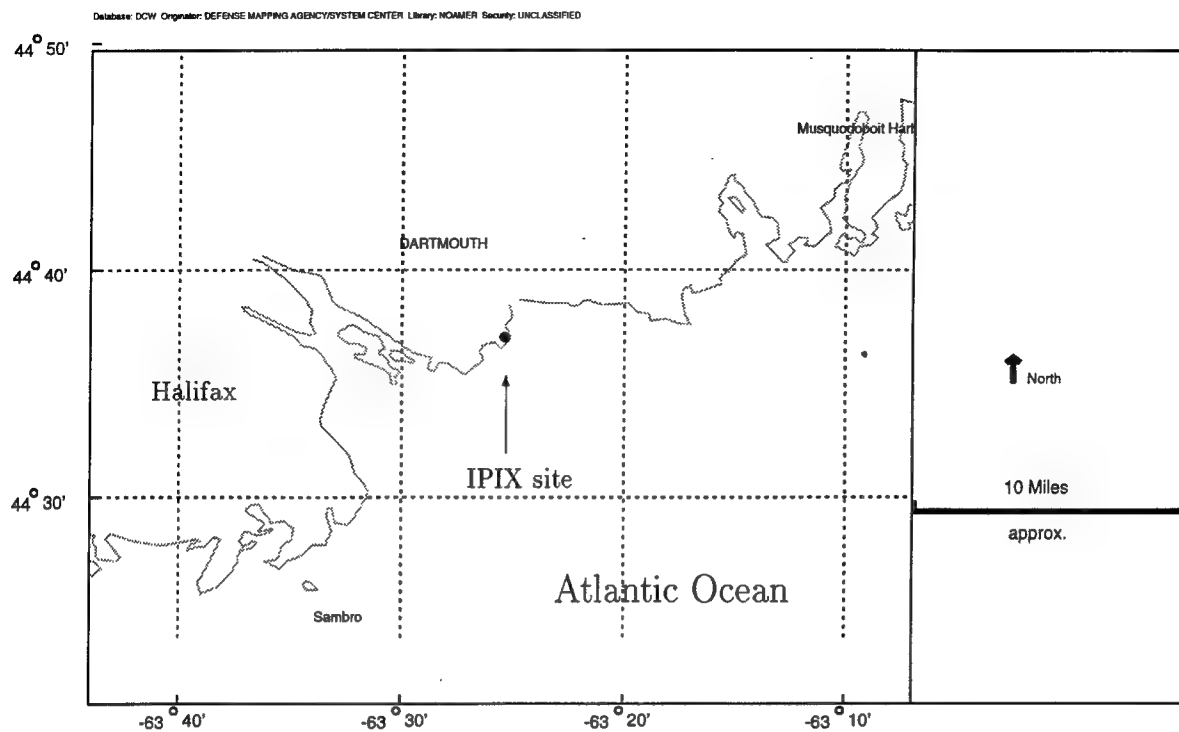
Figure 1.1: The IPIX radar site at Osborne Head Gunnery Range (OHGR). Extracted from "Digital Chart of the World", Ed. 1, July 1992, North America CD database, United States Defense Mapping Agency.
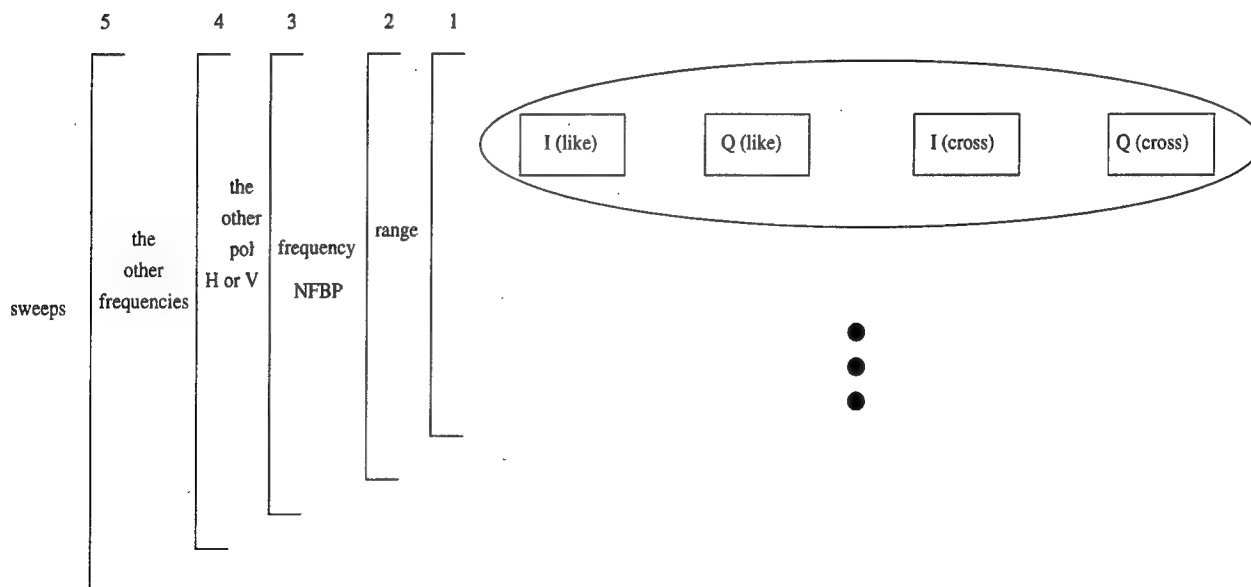
Figure 1.2: The data order of the OHGR datasets.

4

When there are two polarizations transmitted alternatively, the maximum polarization switching rate is 4 kHz. Hence, for high PRF's, for the multi-frequency datasets, a number of different frequencies (NFBP) were transmitted before polarization switching (Loop 2). For example, for a total of four frequencies and NFBP=2, the sequence would be:

Xmt pol	freq
H	f1
H	f2
V	f1
V	f2
H	f3
H	f4
V	f3
V	f4
H	f1
⋮	⋮

If the dataset is not multifrequency or if the PRF is low enough that NFBP=0, there is no loop 2 in the data structure. Loop3 repeats the inner loops with a different transmit polarization for the dual polarized datasets. If the dataset is collected with a single polarization this loop does not exist. Loop 4 repeats the inner loops for a different frequency, i.e. previous frequency incremented by the frequency step. If the dataset is not multifrequency this loop does not exist. Finally, loop 5 repeats the inner loops for all data sweeps. The sweeps are in time only if the dataset is a stare dataset (antenna is staring in a single direction) or in time and azimuth for a scan dataset (antenna is scanning).

The integer data must be scaled from [0,255] to $[-0.7, 0.7]$ where the latter range is in volts. The DC offsets for each of the 4 I/Q channels should then be removed as well. The simplest way to do this is to estimate the mean value of each channel and extract it, assuming the background noise is zero-mean.

If desired, the data can be calibrated to dB_{sm}. The procedure for point targets such as the dihedral and trihedral reflectors employed, is to use the formula

$$dB_{sm} = 10 \log_{10}(I^2 + Q^2) + 40 \log_{10}(R/1000) + G$$

where the radar range R is in meters and the gain factor G is derived from the RF and IF STC values:

RF STC (Volts)	IF STC (Volts)	G (dB)
7.5	2.5	31.3
5.0	0.85	12.6
2.5	0.85	0.3
0.0	0.85	−16.8
0.75	0.85	−14.05
1.0	0.85	−11.7
1.1	0.85	−10.86
1.25	0.85	−9.4
1.5	0.85	−7.3
1.75	0.85	−5.4
2.0	0.85	−3.4
2.25	0.85	−1.8

The main goal for the OHGR trials was to collect enough data to enable one to make reasonable inferences about sea clutter statistics. This is the reason that most datasets are staring ones, i.e. long records at a particular azimuth direction. Another objective was to see what advantages a dual polarized and frequency agile system offers. Theoretically, with frequency agility, a high resolution synthetic range profile can be constructed leading to improved range resolution. Finally, a first investigation on higher order non-Gaussian statistics from experimental data is made possible. Preliminary computations of bispectra for target and clutter cells show differences that could be used for target discrimination. These and other ideas are explored in a follow up report.

The only problems that this database has are:

- The signal gain level at the receiver is often not set at the proper level so that data clipping occurs. Depending on the level of clipping and the signal bandwidth, a suitable low-pass filter could reduce the quantization noise that occurs, making usable the "clipped" dataset.

- Often, I and Q imbalances between the in-phase, I, and quadrature-phase, Q, channels exist and a proper IQ calibration procedure should be employed.

The following section discusses in detail a representative dual polarized dataset. A number of other datasets from Nov 5 – 11 are also investigated in a preliminary fashion. Finally, the database itself, including all operational and ground-truthing data (weather and sea surface information from the nearby base at Shearwater) can be made available to interested organizations in the form of 8mm Unix tar archived and compressed tapes.

2

A Stare Dataset Example

The stare example dataset chosen is, Nov11–stare1 (Table 2.2). As with every dataset in the database it is compressed with the GNU gzip program. To uncompress, use

```
gzip -d stare1.dat.gz
```

Both UNIX and DOS executable programs of gzip are provided in the tapes. As a check to proper reading of the data, Table 2.1 shows a selection of byte records.

The first 1200 bytes always represent a header and the last 16 bytes a trailer. At the end of each range sweep there is also a quadruple of 255's to mark the data end. These must be removed.

The raw IQ traces are first extracted for each polarization channel. Figs. 2.1 – 2.2 show the results.

DC bias is evident on all data. To remove this bias and also check if any strong IQ imbalances are present, each range gate time series is Fourier transformed. In Fig. 2.3 the range frequency description of the data is visible. This is similar to the conventional range-doppler processing. Indeed, the target range bin is clearly visible (more so on a superior display monitor). For this dataset there are no IQ imbalances visible. They are therefore assumed negligible and ignored (this may not always be the case). The dc component is extracted as follows: The dc component of each range bin time series is first computed and subtracted. However, in order to not create an artificial notch at zero frequency, the linearly interpolated dc component from the two frequency neighbors for each range bin is added to the data. A more accurate estimate for the dc component that is removed, could be estimated from a number of consecutive range-time traces where no target exists

7

Table 2.1: A selection of byte records

irec	value	irec	value
1	83	1201	140
2	82	1202	133
3	0	1203	121
4	4	1204	132
5	0	1205	139
6	0	1206	133
⋮	⋮	⋮	⋮
1196	7	902316	131
1197	0	902317	255
1198	13	902318	255
1199	192	902319	255
1200	0	902320	255
		⋮	⋮

Table 2.2: Parameters for the Nov11-stare1 dataset

dataset	Nov11-stare1
number of range samples n_r	54
number of time sweeps n_s	4096
start range r_s	2001 m
range sampling rate SR_r	10 MHz
PRF	400 Hz
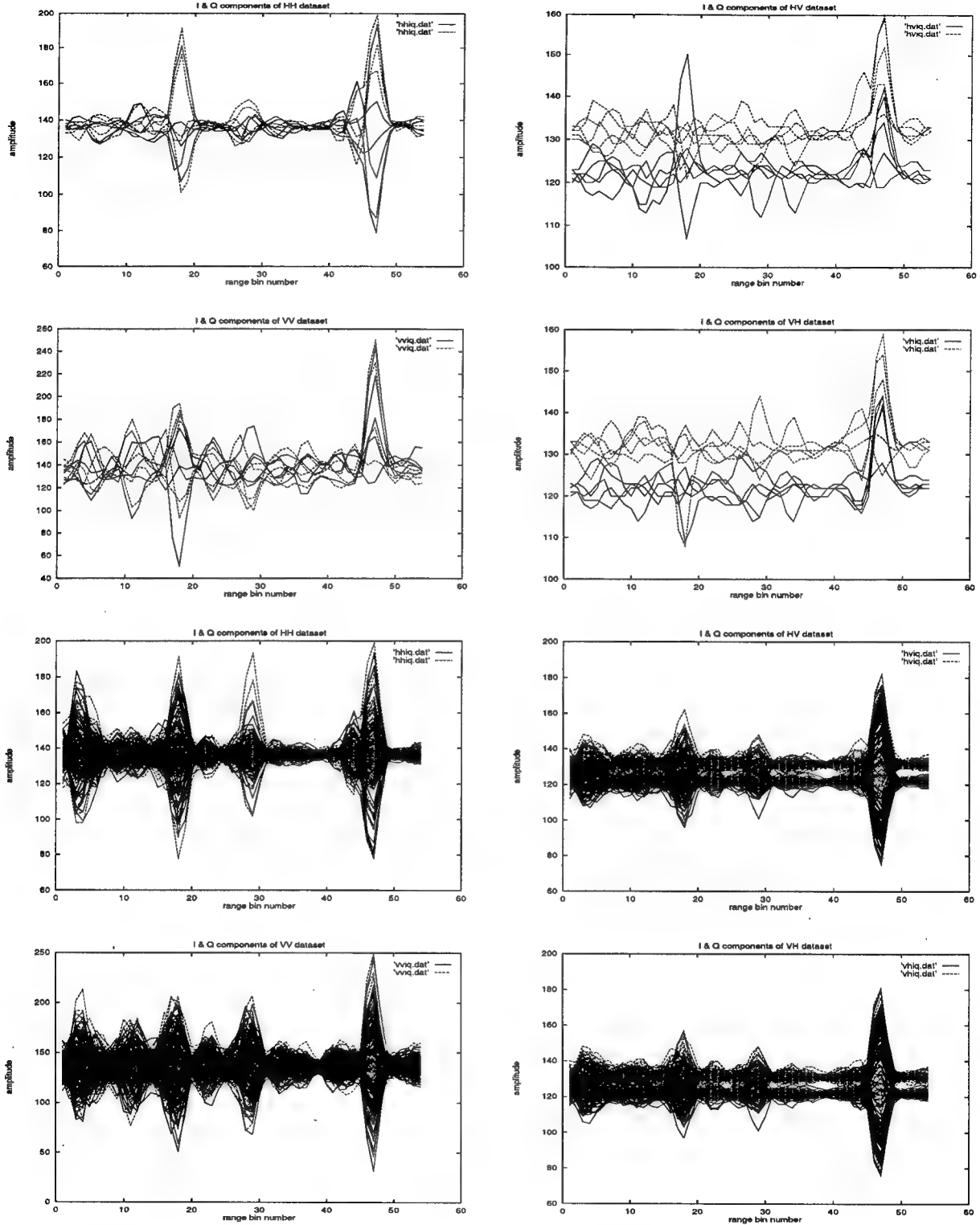
Figure 2.1: Nov11–stare1 dataset. The raw I and Q data. The top four graphs are for the first 5 sweeps only. The quantization errors seem to be small. Data clipping does not seem to be a problem for this dataset. The lower four graphs are for 100 sweeps superimposed. DC bias is seen to be present. The target is visible at range bin 47 or range 2690 km. However, sea clutter also gives strong peaks and the target designation is made based on a priori knowledge of its range.

9
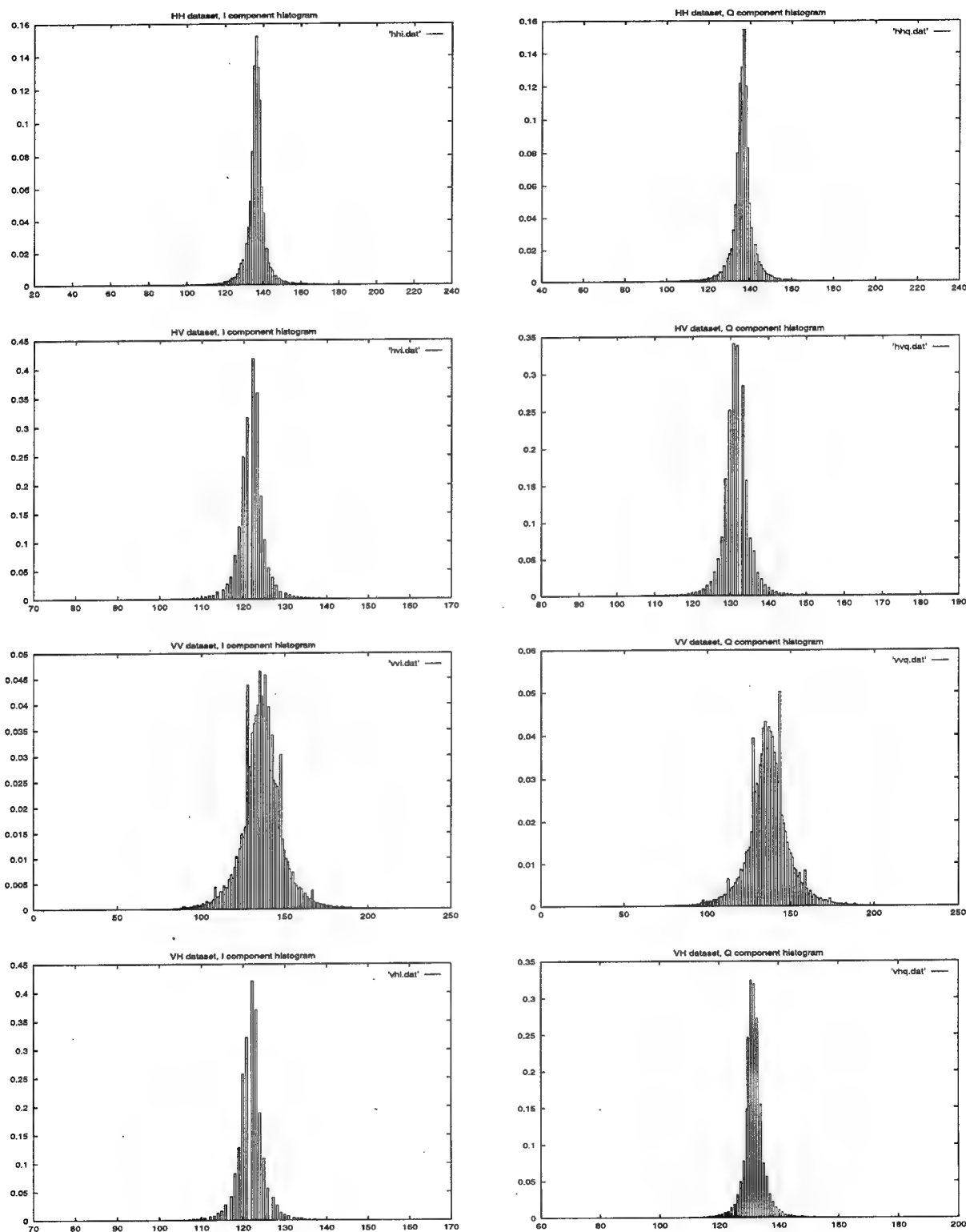
Figure 2.2: Nov11–stare1 dataset. Histograms of the raw I and Q data for the entire dataset. Some minor data clipping is evident on the cross channels.
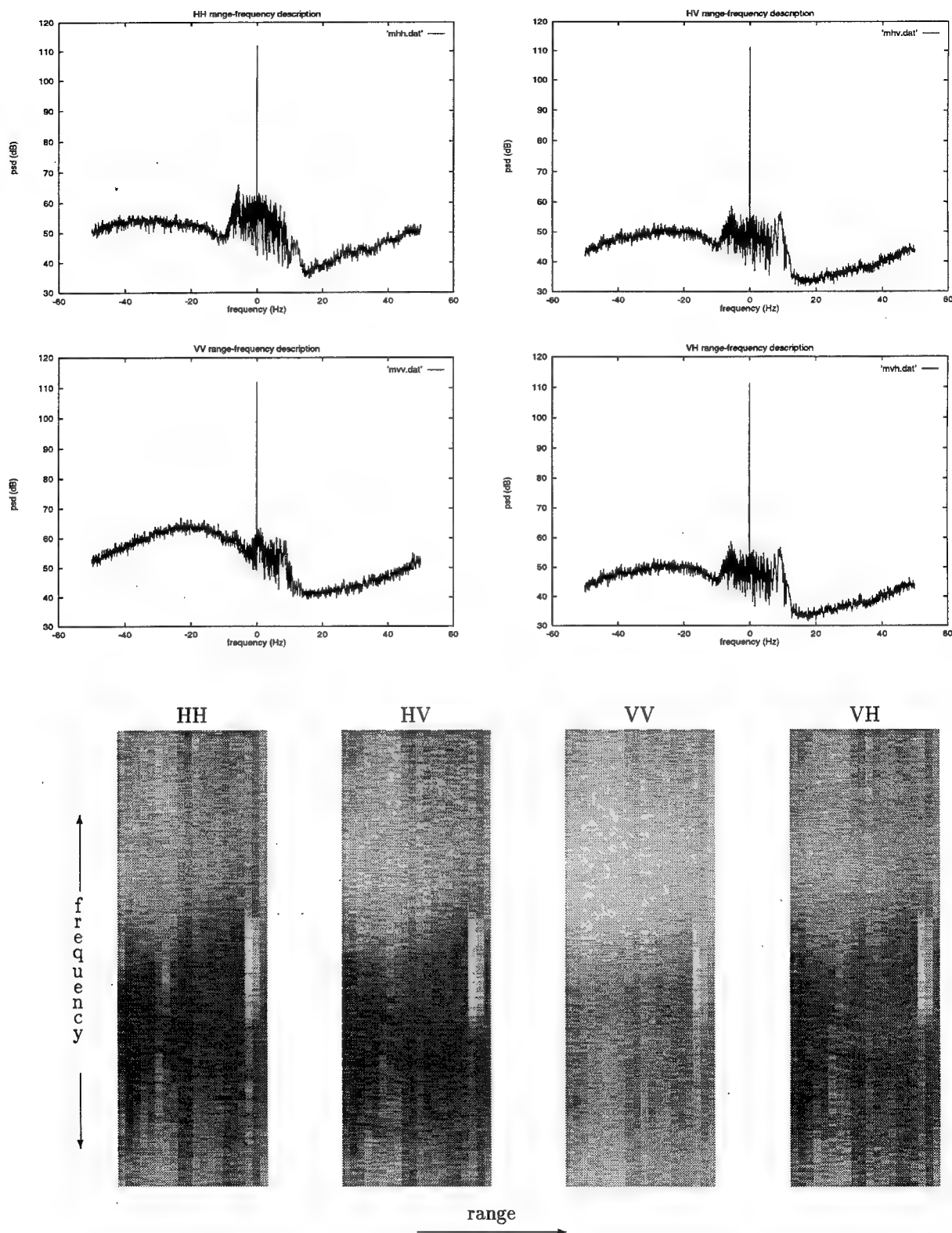
Figure 2.3: Nov11–stare1 dataset. Range-frequency description. The top four graphs display the average frequency description, averaged over all ranges. Note that the "bump" in the middle is the contribution from the target range bins. Note also the 'sinusoidal' wavelike variation of clutter. Aliasing seems to be present due to the small bandwidth available for this dataset. The bottom images are after the DC removal, and the target range bin is clearly evident.

11

(it is assumed that clutter is a zero-mean stochastic process), or from datasets where the Xmtr is off. This is not done here. Another possibility is to estimate the complex average of the entire dataset and subtract it from the data. Indeed, this simpler procedure was carried out for the scanning datasets.

The scan average over time is shown in Fig. 2.4 and the amplitude images in Fig. 2.5. Both are for dc corrected data. The scan average is capable of picking out the target. In the amplitude images however, this is not so clear. Note the higher clutter level in the VV channel. Note also the differences in the amplitude histograms in Fig. 2.4.

Time–frequency images of selected range bins can also be computed. Fig. 2.6 demonstrates the difference between a target and clutter bin. The sinusoidal-like behavior for the target bin, displays the interaction of the buoy target with the wave motion of the ocean. Note also the appearance of a distinct clutter band in the negative frequencies. i.e. receding ocean waves.
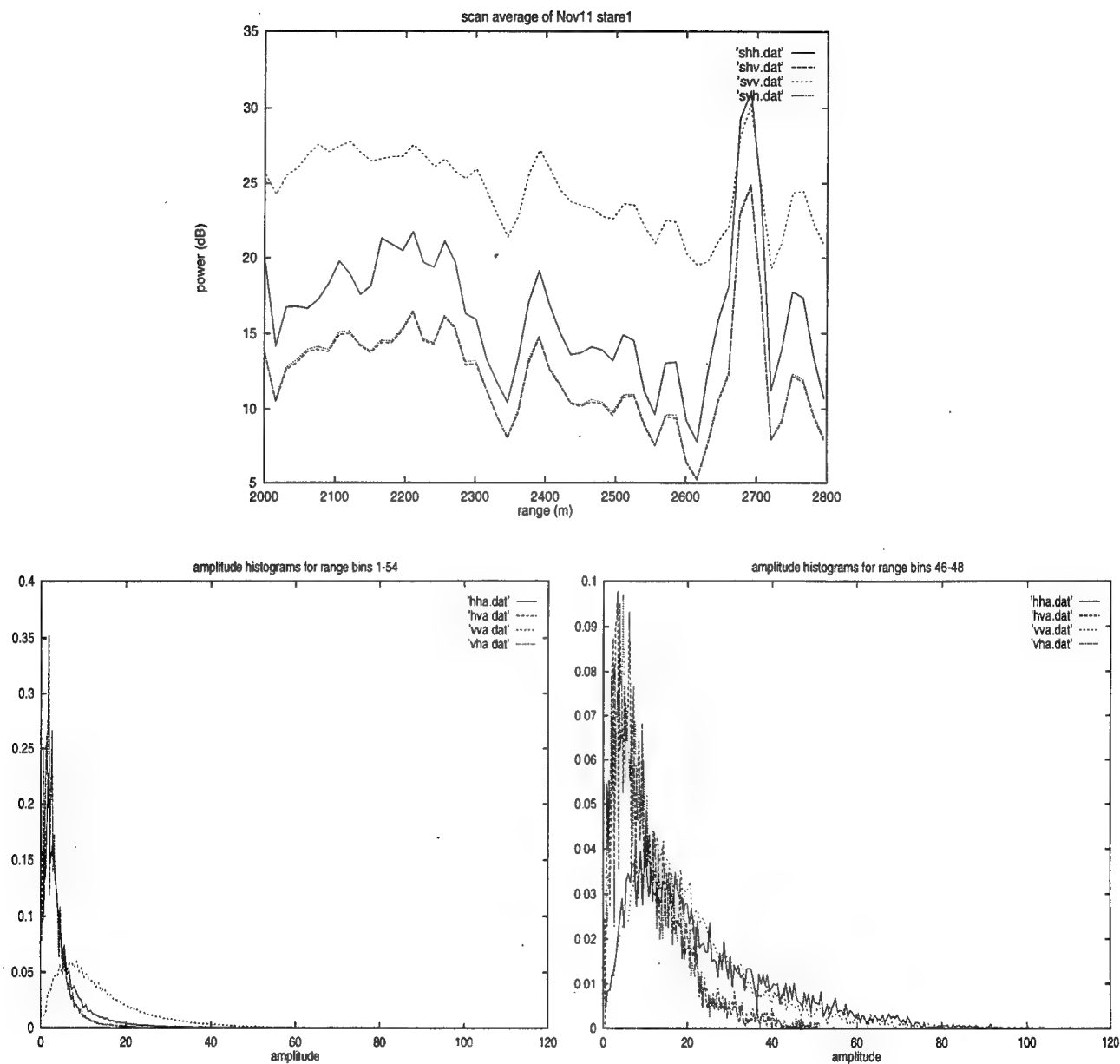
Figure 2.4: Nov11–stare1 dataset. The scan average over time (top graph). The target is seen to be at range 2690m. The two bottom graphs display the amplitude histograms. The left one is for the entire dataset, all range bins, while the the right one is only for bins 46-48 which contain the target. Note the differences.

HH HV VV VH

t
i
m
e
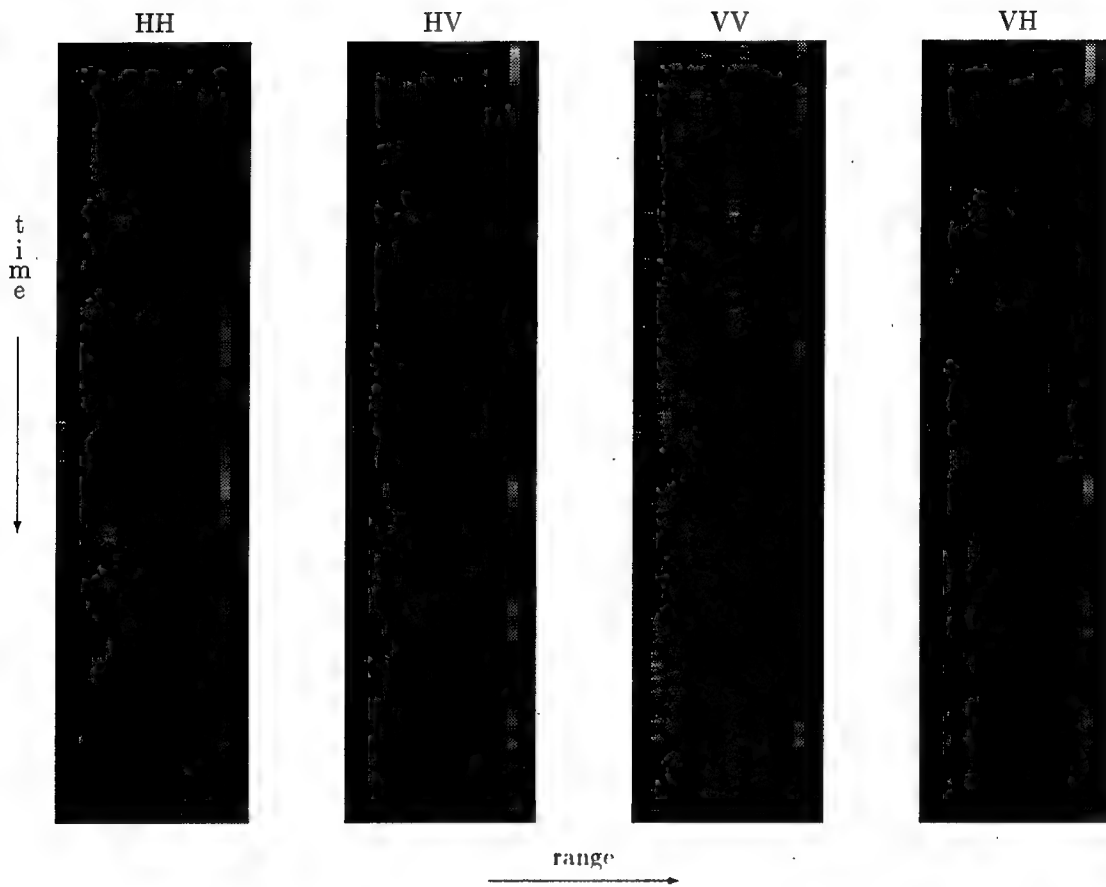
range

Figure 2.5: Nov11–stare1 dataset. The corresponding amplitude images. Note the more wavelike behavior of the VV channel.
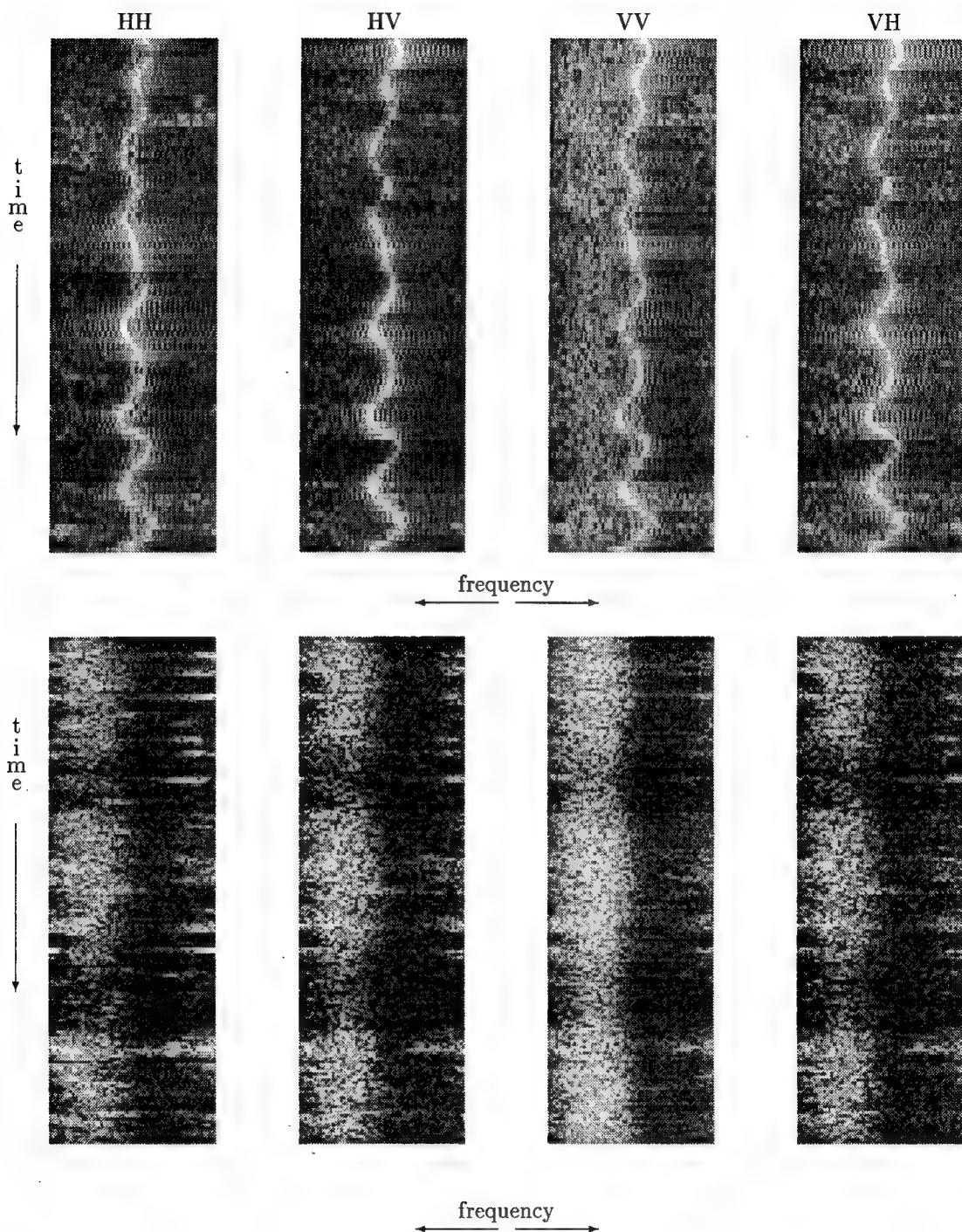
Figure 2.6: Nov11–stare1 dataset. Time-frequency images for the target range bin 47 (top four), and the clutter range bin 10 (bottom four). A 32-point sliding FFT with 25% overlap was employed. The frequency ranges from −50 to 50 Hz and time from 0 to about 10 sec.

15

3

Nov5 datasets

The datasets collected are given in Table 3.1

An individual description:

Starea0 Severe clipping, evident both in the raw IQ traces and histograms. Slightly better for the cross polarized channels. The azimuth direction is that of the dihedral and trihedral targets. They appear more clearly on the cross pol data. A rather consistent notch is also evident. The time range amplitude images suggest that the antenna or targets were moving slightly. Some IQ imbalances are present as well.

Starea1 Much better. Negligible clipping. Some IQ imbalances.

Starea2 Good. Some slight clipping on like pols, negligible on xpols. Some IQ imbalances. The

Table 3.1: Nov5 datasets

	time	dataset	pol	PRF kHz	n_r	SRR MHz	r_s m	n_s	Az $^\circ$		El $^\circ$	rpm
1	0832	starea0	alt	1	68	25	2199	1024		223.528	−0.291	
2		starea1								223.518	−0.295	
3		starea2								223.627	−0.297	
4	0842	surv0	H	0.8	251	25	1500	1112	200.006	252.268	−0.403	6
5		surv1							199.990	252.164	−0.313	
6		surv2							200.045	252.043	−0.192	
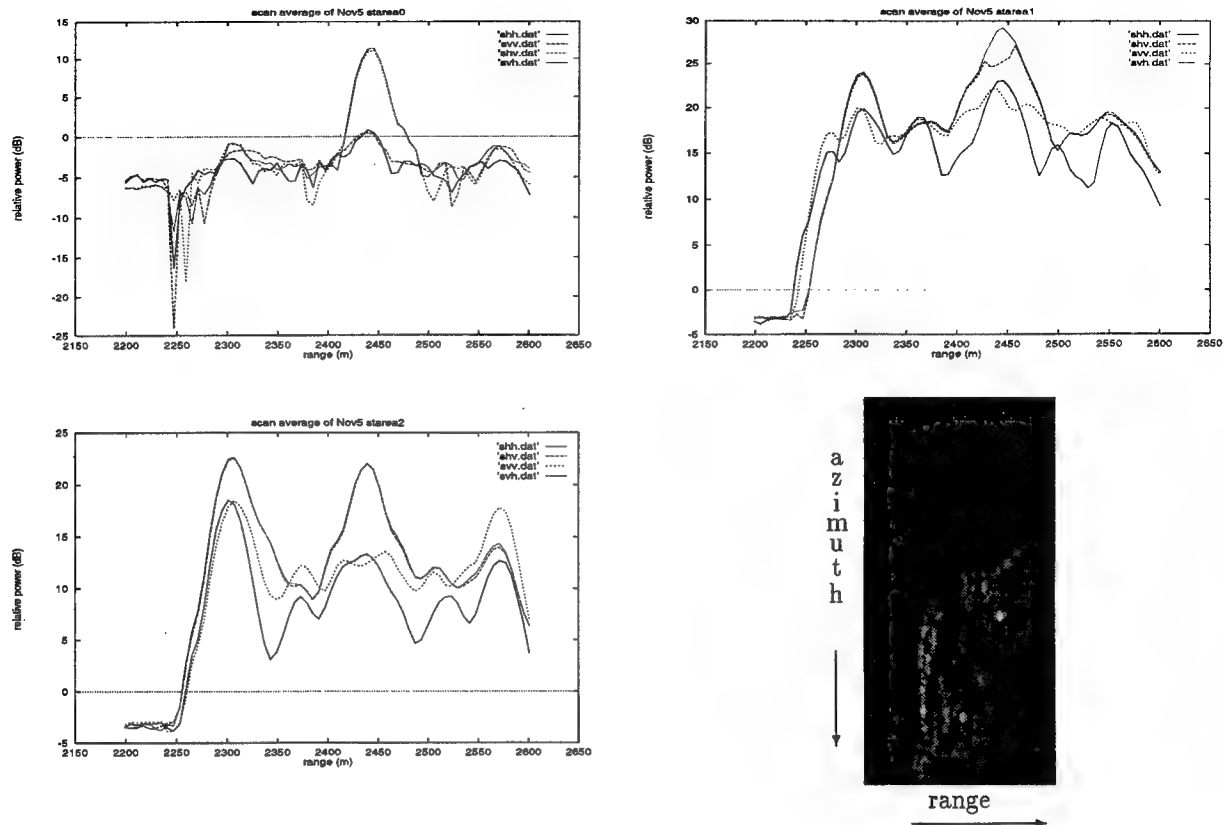
Figure 3.1: Scan averages of the stare data. Note the difference between like and cross polarization signals. Despite the severe clipping, the Bscan of surv2 at the bottom right, shows two bright spots that could be the two reflectors.

trihedral is more evident (look azimuth angle). Another target seems to be evident at the far end. Amplitude images are also interesting with "bright" and "faint" areas.

Surv0 Very bad clipping here. This is a scanning dataset looking over the dihedral & trihedral azimuth sector. Useless.

Surv1 Same.

Surv2 Same. Interestingly enough there are two bright points visible on the Bscan at (2268m, 263.05°) and (2562m, 229.238°). Dihedral and trihedral reflectors ?

17

4

Nov6 datasets

The stare datasets here (Table 4.1) are all multifrequency ones. Only the first frequency subset is investigated. The rest may, or may not be of similar quality. A conversion from Bscan to PPI was done here for the scanning datasets through the cubic convolution interpolation algorithm [1, 3]. The Bscan polar array was converted to a rectangular grid of 500×500 pixels. The amplitude intensity was then scaled to the range [0,255] and written in a Portable Grayscale Map, PGM, ASCII file format. Packages like PBMplus, or XV (the one used here) can do the display and conversion to postscript.

Starea0 No clipping. Looks good. A thin strip with a buoy target in. Range:2150m, bin:6. Have looked at the total 8192 sweeps. Excellent potential for synthetic range reconstruction. The range–frequency description is interesting too. A bright localized target and a much broader clutter band. See Fig. 4.1 the two top images.

Starea1 Some slight clipping. Same as above otherwise.

Starea2 Better. No clipping. No targets clearly visible although there might be something at far right. Nice clutter in range–frequency description.

Starea3 OK. Some slight clipping on xpols. The range–frequency indicates rather severe IQ imbalances.

Starea4 Same as above. IQ imbalances here too. The spread in the range–frequency description is around dc, indicating a calmer sea. The amplitude histograms seem to be more K-distributed than in starea3.

Table 4.1: Nov6 datasets

	time	dataset	pol	PRF kHz	n_r	SRR MHz	r_s m	n_s	n_f	Az °		El °	rpm
1	1215	starea0	alt	2	11	5	2001	262144	16	209.818		−0.199	
2		starea1								209.813		−0.200	
3	1340	starea2								211.173		−0.455	
4	1400	starea3								189.988		−0.406	
5	1413	starea4								99.894		−0.406	
6	1418	starea5								144.927		−0.401	
7	1718	starea6			28		11700	131072	8	170.114		−0.214	
8	1130	surv0	H	0.8	184	5	501	8000		26.938	41.292	−0.889	6
9		surv1	V							26.082	359.995	erratic	
10	1431	surv2	H							52.482	63.990	−0.845	

Starea5 Not so good. HH OK, VV slightly clipped, but the xpols severely so. IQ imbalances. The range–frequency peak has shifted to the right.

Starea6 The number of range gates and their coverage is changed. Have 4096 time sweeps. Quite good regarding clipping. IQ imbalances similar as above. Two target buoys clearly visible at 11880m and 12330m. A pity only 4096 sweeps per frequency are available. Not enough to see a full cycle on a range–doppler image.

Surv0-2 O.K. as far as it goes. IQ histograms show negligible clipping and the PPI image is typical of all. Note however that the azimuth is erratic on surv1 (Fig. 4.2).
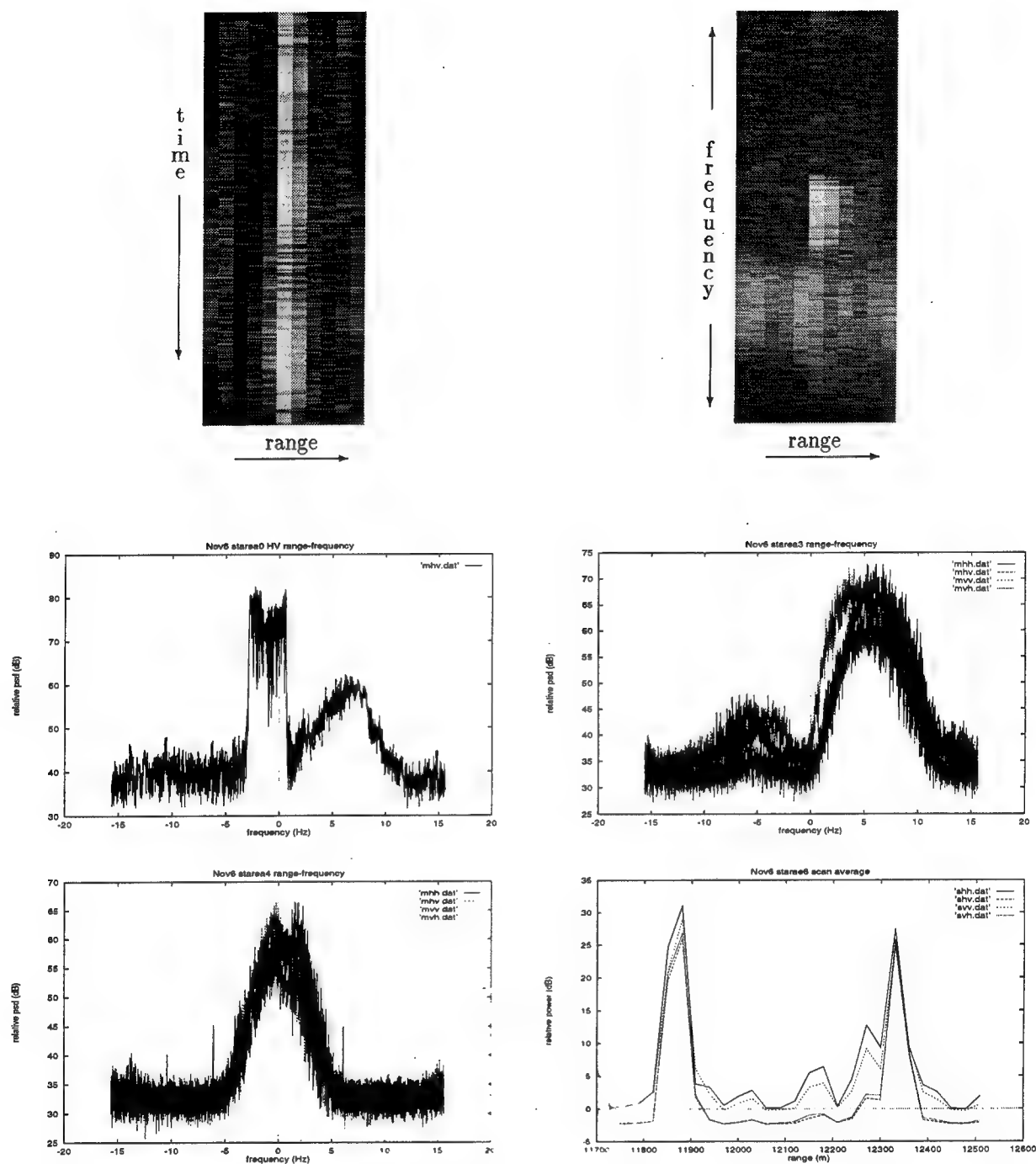
Figure 4.1: The two top images are the HH-amplitude, time-range and frequency-range plots of starea0. The middle left graph is another view of the frequency-range plot for the HV polarization, where the range is averaged out. In this case, the target and clutter spectra are nicely separated. The middle right graph is for starea3 where there is no target. For starea4, where the sea state seems to be calmer, the clutter spectrum occupies the same bins as any slow moving target would and no separation based on this approach is possible. Finally, the scan-average of starea6 clearly shows the two marine target buoys.

20

Bscan

PPI

azimuth
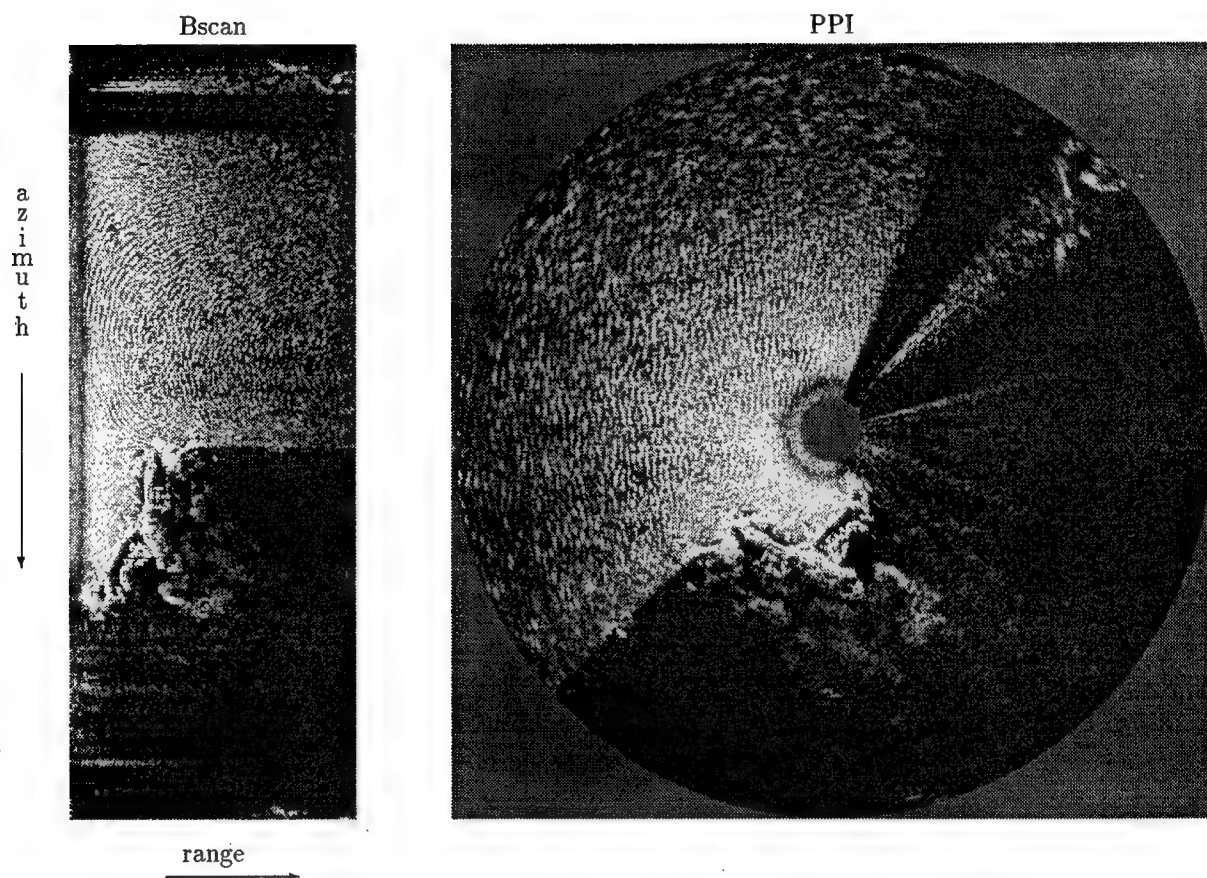
range

Figure 4.2: The Bscan and PPI images for surv0, HH pol. The range varies from 500m to 6km.

21

5

Nov7 datasets

The stare datasets here are again multifrequency ones (Table 5.1). Only the first frequency subset is investigated.

Starea1 No clipping visible on the like polarized channels. Looks good. Some slight clipping on the cross polarized channels. A thin strip of data with 2 targets? in. The second one seems more solid and clearly identified as the only target from the range–frequency plots. Sea conditions seem to be calm, leading to target and clutter occupying the same frequency bins. On the range–doppler plot (not shown here) the target trace is practically a straight line. The target is brighter and can easily be picked out in the range–frequency plots. Some IQ spikes are evident there as well.

Starea2 Clipping is very bad here. Useless.

Table 5.1: Nov7 datasets

	time	dataset	pol	PRF kHz	n_r	SRR .MHz	r_s m	n_s	n_f	Az °		El °	rpm
1	0953	starea1	alt	2	14	10	2574	262144	16	128.881		−0.302	
2	1013	starea2								128.877			
3	1047	starea3								130.395			
4	1123	starea4								133.878		−0.305	
5	1159	starea5								155.764		−0.209	
6	0925	surv0	H	0.8	468	10	999	1890		139.966	227.390	−0.297	6
7	0930	surv1	H							140.004	227.477	−0.296	

Starea3 Same here.

Starea4 Only the VV channel is OK. Others as bad as above.

Starea5 Clipping is less severe. The dataset is usable. There is a small boat target, practically standing still at range 6174 m and it is interesting to see the amplitude and range frequency images. From the frequency shift $f_d = 2.5$ Hz one can calculate the radial velocity of the boat with respect to the radar (closing target) from

$$v_r = \frac{c f_0}{2 f_d}$$

to be $v_r = 0.04$ m/s, where $f_0 = 9.39$ GHz the carrier frequency and c is the speed of light.

Surv0 Looks OK.

Surv1 Same here.
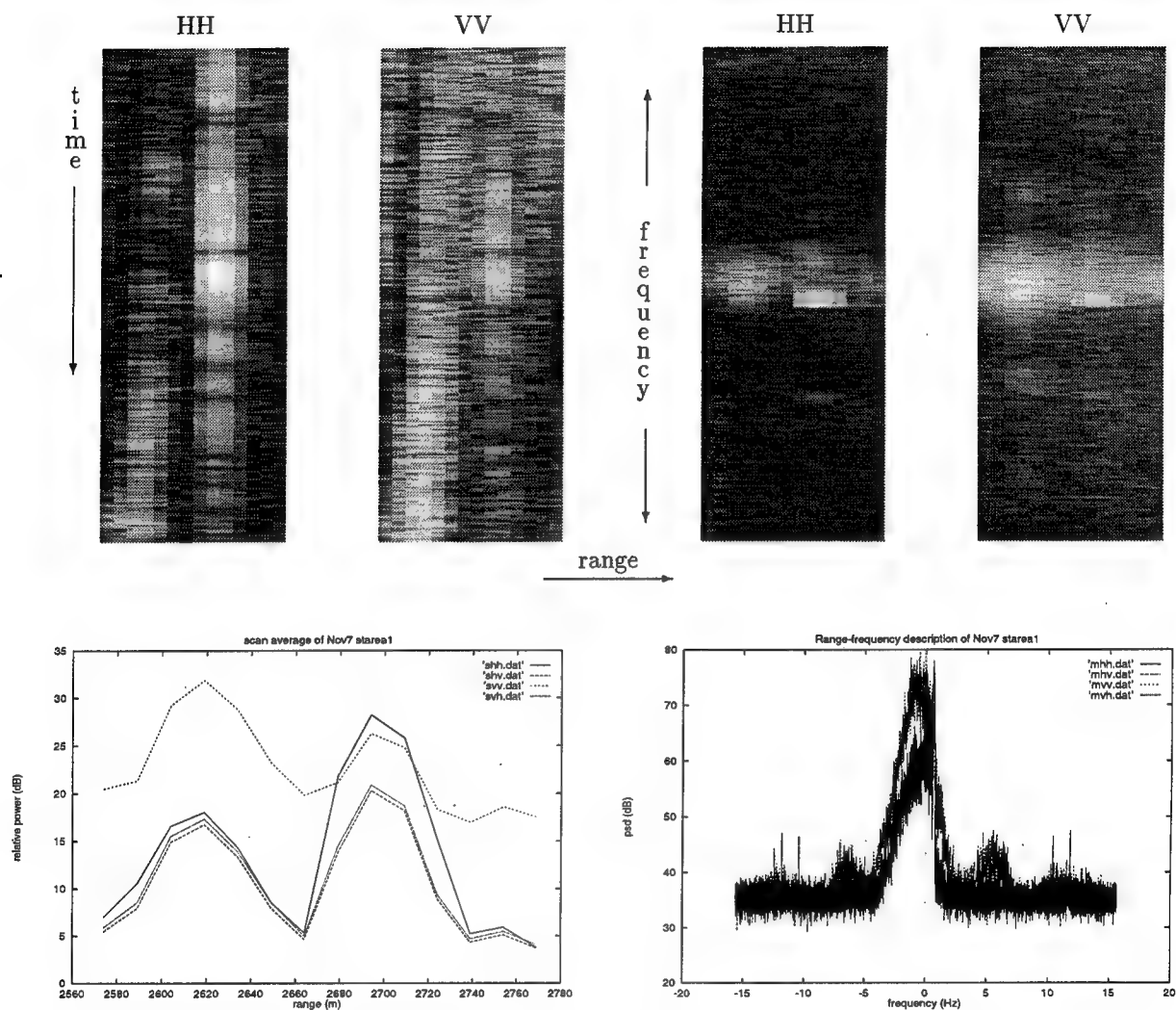
Figure 5.1: The two top left images are the HH and VV amplitude images of starea1. The two top left ones are the corresponding frequency–range plots. The bottom left is the scan average of the amplitudes and the right is the frequency–range image averaged over range.
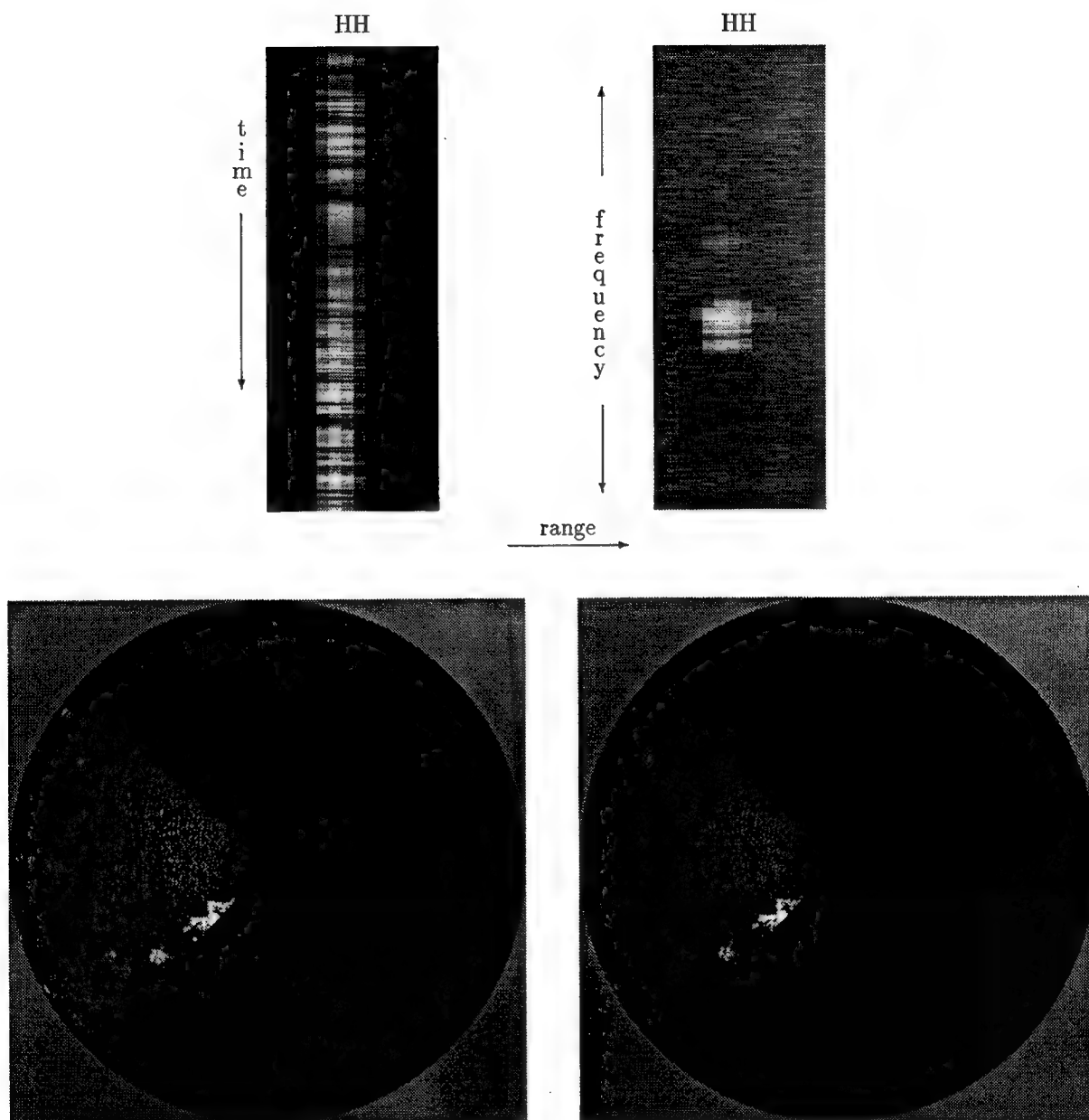
Figure 5.2: The two top images are the HH amplitude, time–range, and frequency–range images of starea5. This is the dataset where a small boat is a closing target. From the first image, the range can be determined and from the second the radial velocity. The two bottom PPI images are for the like and cross polarized channels of surv0. Surv1 is similar.

6

Nov8 datasets

The stare datasets here are again multifrequency ones (Table 6.1) and only the first frequency subset is investigated.

Starea0 Target A is supposed to be visible here. Data clipping is bad, however. The scan average indicates three targets at 2600, 2660 and 2720 m with the last one being strongest. Useless.

Starea1 Much better. No clipping here. Target A is clearly visible at 2660 m in the scan average. Interestingly enough it is much harder in the amplitude images although somewhat easier in the range–frequency ones (Fig. 6.1).

**Starea2** Good. Similar to above except that it is looking purely on clutter.

Surv1 There was radar interference from the OHGR radar. It is interesting to see what it looks like in the Bscan (Fig. 6.2).

Table 6.1: Nov8 datasets

	time	dataset	pol	PRF kHz	n_r	SRR MHz	r_s m	n_s	n_f	Az °		El °	rpm
1	1726	starea0	alt	2	14	10	2574	262144	16	127.072		−0.308	
2	1804	starea1								127.067			
3	1853	starea2								189.969			
4	1000	surv1	H	0.2	528	2	501	1112		60.178	264.326	−0.220	6
5	1334	surv2	H		251	5	501			60.233	264.304	−0.438	6
6	1334	surv3	H							60.304	265.100	−0.359	

Surv2 Good. PPI image in Fig. 6.2).

Surv3 Good here too.
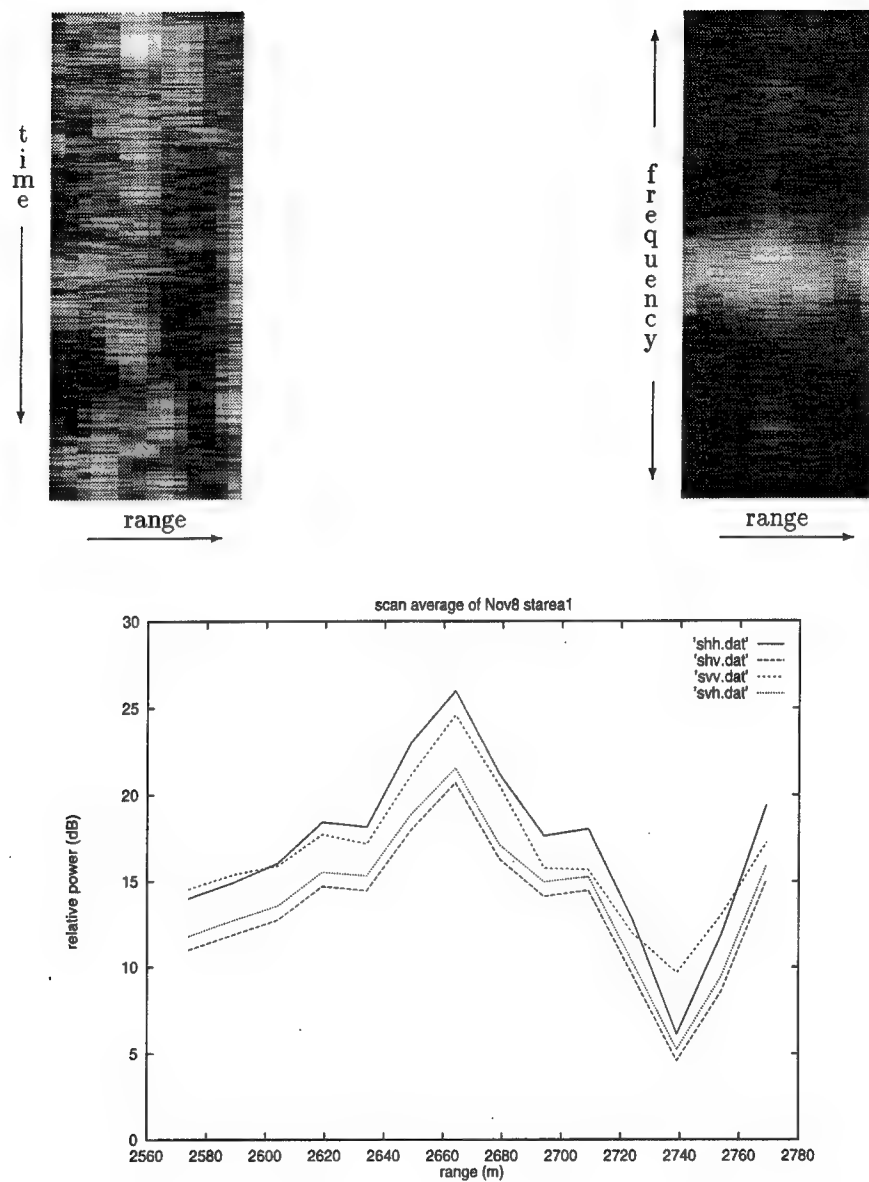
Figure 6.1: The two top images are the HH-amplitude, time–range and frequency–range plots of starea1. The bottom graph is the scan average, i.e. average over time of the time-range amplitude plot.
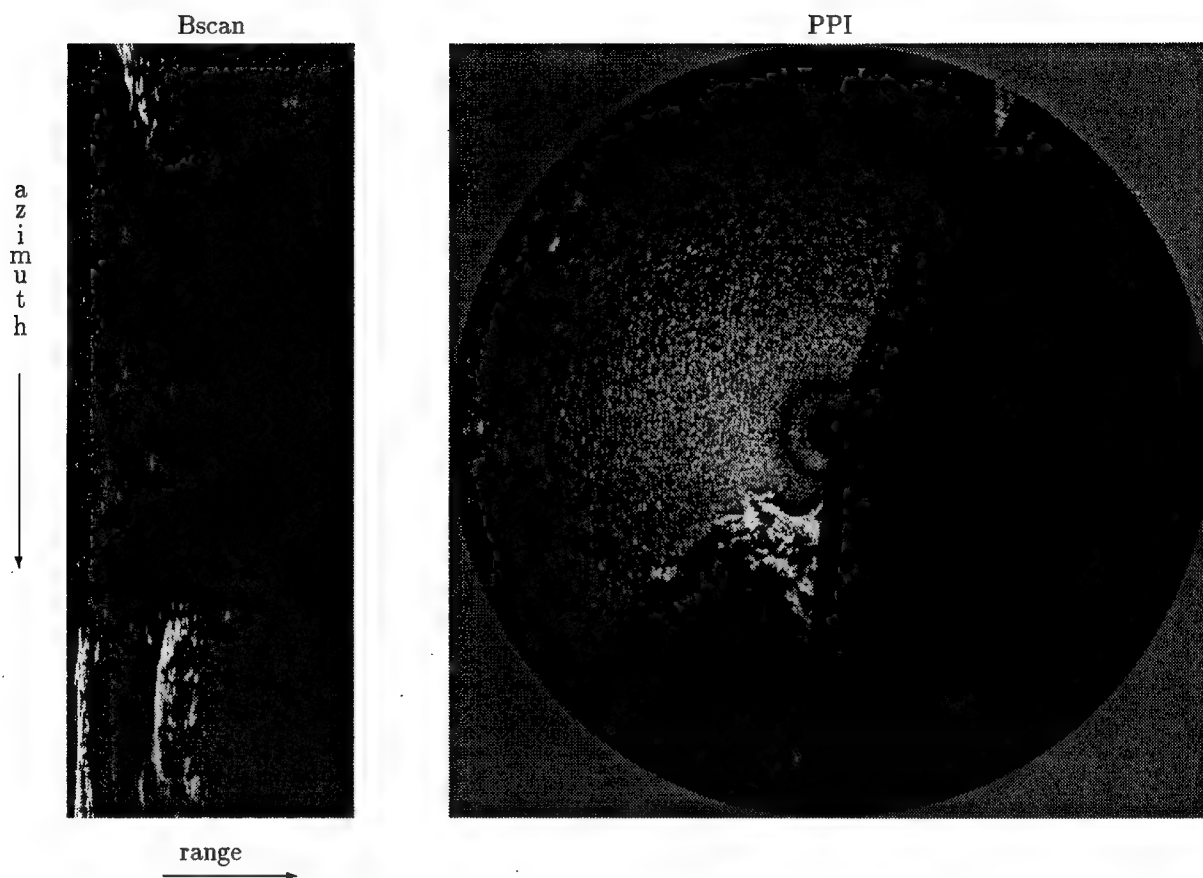
28

Bscan

PPI

a
z
i
m
u
t
h

range

Figure 6.2: The Bscan of HH pol surv1 on the left. Note the OHGR radar interference spots appearing as black rectangles at near range. The PPI of surv2 is on the right. Surv3 is similar to surv2.

7

Nov11 datasets

Four small alt polarized datasets are investigated here (Table 7.1). The first two are similar to the one used in the stare dataset example and the other two are looking at the dihedral and trihedral reflectors.

Stare0 Target at 2700m and no clipping. Good.

Stare2 Rather severe clipping. Target B is supposed to be visible around 5600m and a weak target seems to be visible there.

Refl0 Good regarding clipping. The histograms clearly show a bimodal distribution and the two reflectors are clearly seen in both the amplitude and scan average images. Note the peaks in the frequency description. These datasets could be used for IQ calibration.

Refl1 Similar to refl0.

Table 7.1: Nov11 datasets

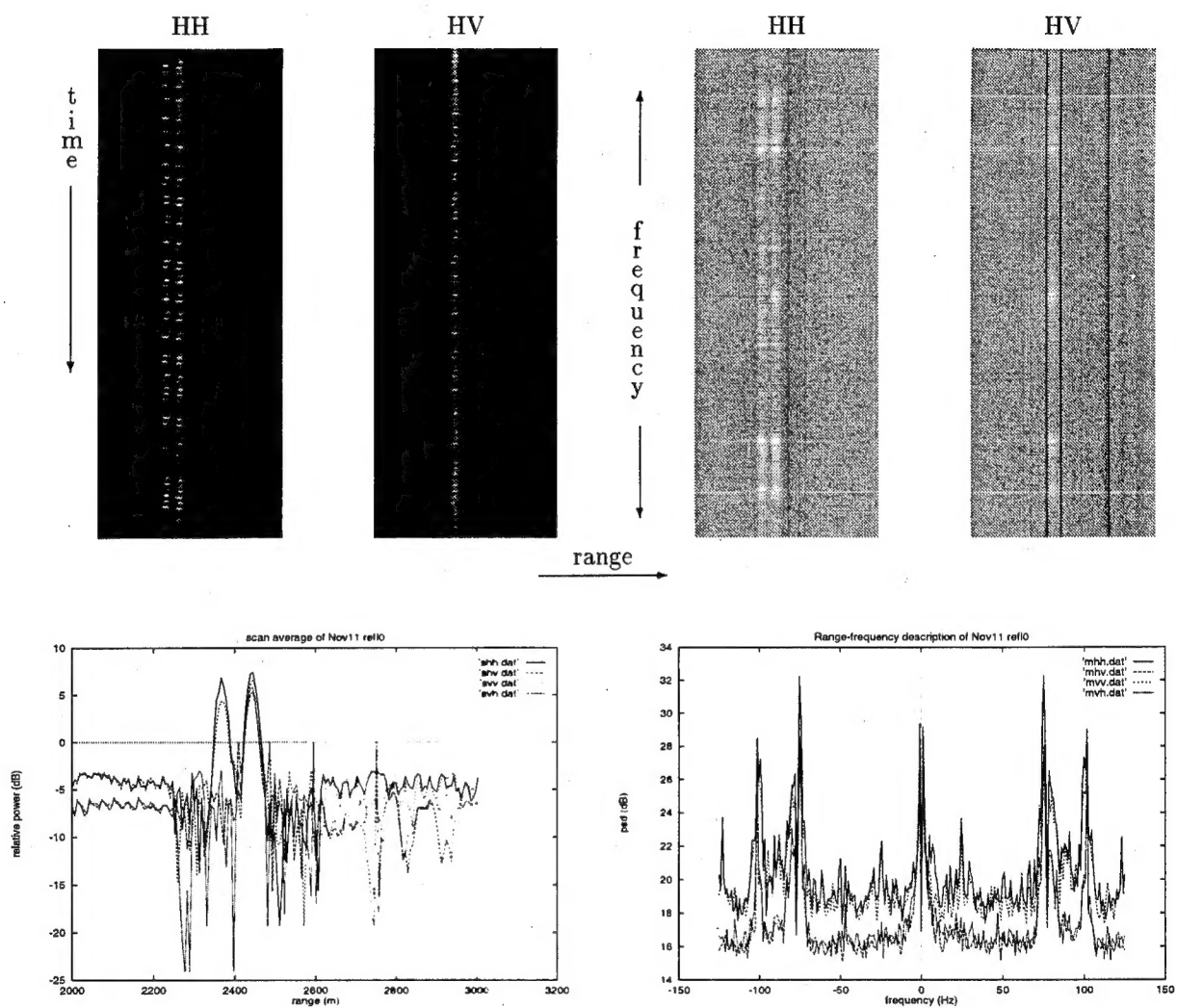|	time	dataset	pol	PRF kHz	n_r	SRR MHz	r_s m	n_s	n_f	Az °	El °	rpm
1	1209	stare0	alt	0.4	54	10	2001	4096	1	129.500	−0.494	
2	1229	stare2					5100			130.281	−0.313	
3	1640	refl0		1	168	25	2001	512		223.149	−0.511	
4	1642	refl1								223.654		

Figure 7.1: The two top left images are the HH and HV amplitude images of refl0. The two top right ones are the corresponding frequency-range imags. The bottom left is the scan average of the amplitudes and the bottom-right is the frequency-range averaged over range.

References

[**1**] A. Damini. *Digital Scan Conversion Algorithms for Ground–Based and Airborne Radars.* DREO Technical Report 1113, Defence Research Establishment Ottawa, 1991.

[**2**] K. Hasselmann, W. Munk and G. MacDonald. *Bispectra of Ocean Waves.* In M. Rosenblatt, editor, *Proceedings of the Symposium on Time Series Analysis*, Ch. 8, pgs. 125–139, John Wiley, 1963.

[**3**] R.G. Keys. *Cubic Convolution Interpolation for Digital Image Processing, IEEE Trans. on Acoustics Speech & Signal Processing*, **29** (1981) 1153–1160.

SECURITY CLASSIFICATION OF FORM
(highest classification of Title, Abstract, Keywords)

DOCUMENT CONTROL DATA
(Security classification of title, body of abstract and indexing annotation must be entered when the overall document is classified)

1. ORIGINATOR (the name and address of the organization preparing the document. Organizations for whom the document was prepared, e.g. Establishment sponsoring a contractor's report, or tasking agency, are entered in section 8.)	2. SECURITY CLASSIFICATION (overall security classification of the document. including special warning terms if applicable)
Defence Research Establishment Ottawa 3701 Carling Ave Ottawa, Ontario, Canada, K1A 0K2	UNCLASSIFIED

3. TITLE (the complete document title as indicated on the title page. Its classification should be indicated by the appropriate abbreviation (S,C or U) in parentheses after the title.)

Description of the OHGR Database (U)

4. AUTHORS (Last name, first name, middle initial)

Drosopoulos, Anastasios

5. DATE OF PUBLICATION (month and year of publication of document) December 1994	6a. NO. OF PAGES (total containing information. Include Annexes, Appendices, etc.) 32	6b. NO. OF REFS (total cited in document) 3

7. DESCRIPTIVE NOTES (the category of the document, e.g. technical report, technical note or memorandum. If appropriate, enter the type of report, e.g. interim, progress, summary, annual or final. Give the inclusive dates when a specific reporting period is covered.)

DREO Technical Note

8. SPONSORING ACTIVITY (the name of the department project office or laboratory sponsoring the research and development. Include the address.)

Defence Research Establishment Ottawa
3701 Carling Ave
Ottawa, Ontario, Canada, K1A 0K2

9a. PROJECT OR GRANT NO. (if appropriate, the applicable research and development project or grant number under which the document was written. Please specify whether project or grant) 021LA	9b. CONTRACT NO. (if appropriate, the applicable number under which the document was written)
10a. ORIGINATOR'S DOCUMENT NUMBER (the official document number by which the document is identified by the originating activity. This number must be unique to this document.) DREO Technical Note 94-14	10b. OTHER DOCUMENT NOS. (Any other numbers which may be assigned this document either by the originator or by the sponsor)

11. DOCUMENT AVAILABILITY (any limitations on further dissemination of the document, other than those imposed by security classification)

(X) Unlimited distribution
( ) Distribution limited to defence departments and defence contractors; further distribution only as approved
( ) Distribution limited to defence departments and Canadian defence contractors; further distribution only as approved
( ) Distribution limited to government departments and agencies; further distribution only as approved
( ) Distribution limited to defence departments; further distribution only as approved
( ) Other (please specify):

12. DOCUMENT ANNOUNCEMENT (any limitation to the bibliographic announcement of this document. This will normally correspond to the Document Availabilty (11). However, where further distribution (beyond the audience specified in 11) is possible, a wider announcement audience may be selected.)

SECURITY CLASSIFICATION OF FORM

DCD03 2/06/87

13. ABSTRACT (a brief and factual summary of the document. It may also appear elsewhere in the body of the document itself. It is highly desirable that the abstract of classified documents be unclassified. Each paragraph of the abstract shall begin with an indication of the security classification of the information in the paragraph (unless the document itself is unclassified) represented as (S), (C), or (U). It is not necessary to include here abstracts in both offical languages unless the text is bilingual).

This Technical Note describes the Osborne Head database, collected at Osborne Head Gunnery Range, OHGR, in November 1993, with the McMaster University IPIX radar, under contract to DSS. Representative examples are worked out for the different operational modes of the radar (staring, scanning, alternate/single polarization, single/multi frequency). Strengths and weaknesses of the database are pointed out as well. The purpose of this Technical Note is to serve as a guide to the database, presenting enough information to allow the extraction of individual datasets from the raw data. These can subsequently be used for sea clutter, target model validation and/or testing of signal processing techniques, leading to enhanced target detection in sea clutter.

14. KEYWORDS, DESCRIPTORS or IDENTIFIERS (technically meaningful terms or short phrases that characterize a document and could be helpful in cataloguing the document. They should be selected so that no security classification is required. Identifiers, such as equipment model designation, trade name, military project code name, geographic location may also be included. If possible keywords should be selected from a published thesaurus. e.g. Thesaurus of Engineering and Scientific Terms (TEST) and that thesaurus-identified. If it is not possible to select indexing terms which are Unclassified, the classification of each should be indicated as with the title.)

Radar Database Description